Latin American Journal of Solids and Structures
www.lajss.org

# Tracking control of a planar five-link bipedal walking system with point contact, considering self-impact joint constraint by adaptive neural network method


## Abstract

In order to achieve the practical characteristics of natural bipedal walking, a key feature is to realize "the straight knee state of walking" during stance and swing motions. Considering a straight knee necessitates that the shank link of each leg not to undergo the rotation angles which are greater than that of the thigh link. For this purpose, various methods have been proposed; the joint self-impact constraint has been suggested for energy-efficient (natural) bipedal walking while realizing the straight knee constraint.

The prominent objective of this research is to present a model based control method for trajectory tracking of a normal human-like bipedal walking, by considering the joint self-impact constraint. To achieve this objective, the dynamical equations of motion of an unconstrained biped are taken, developed and then modified to consider the joint self-impact constraint at the knee joint.

To control this complicated dynamical system, the available anthropometric normal gait cycle data are taken to generate the desired trajectories of the thigh and knee joints of the self-impact biped. Due to the existence of complex nonlinear terms in the dynamical governing equations of self-impact biped, the authors propose to design a nonlinear intelligent controller by taking advantage of the adaptive neural network control method, which neither requires the evaluation of inverse dynamical model nor the time consuming training process. According to the simulation results, the tracking control of the biped robot is accomplished well and the biped walking seems naturally, despite of involving complex nonlinear terms in the dynamical governing equations of the self-impact biped.



## Keywords

Leg locomotion; self-impact constraint; biped; dynamical modeling; adaptive neural network.



Yousef Bazargan-Lari[a]
Mohammad Eghtesad[b*]
Ahmad Reza Khoogar[c]
Alireza Mohammad-Zadeh[d]

[a,d]Department of Mechanical Engineering, Science and Research Branch, Islamic Azad University, Tehran, Iran
[a]bazarganlari@iaushiraz.ac.ir
[d]mohammadzadeh2001@yahoo.com
[b]School of Mechanical Engineering, Shiraz University, Shiraz, Iran
[c]Department of Mechanical Engineering, Maleke-Ashtar University of Technology Lavizan,Tehran, Iran
[c]khoogar@yahoo.com

Corresponding author:
[b*]eghtesad@shirazu.ac.ir



http://dx.doi.org/10.1590/1679-78251563

Received 18.09.2014
Accepted 24.03.2015
Available online 22.04.2015

## 1 INTRODUCTION

Human locomotion is the ability of human to move from one place to another; it may take place through walking, jogging, and running gaits, which are the three perspectives of the human locomotion. Walking happens more frequently than the other two. It is defined as subsequent gait cycles; each walking gait cycle means the period from initial contact of one foot to the following initial contact of the same foot.

Human locomotion is imitated by biped robots for use under extreme environments and for onerous reiterative works in some industrial fields. Legs are adapted to cluttered environments allowing the machine to stride over obstacles and limiting the damages to the environment thanks to their small support surface (Azevedo et al., 2004). It is known that the mobility of legged mechanisms on rough terrains is better than that of wheels because legs can use isolated footholds to optimize support whereas a wheel requires a continuous path of support. In general, a biped robot consists of several links that are interconnected by actuated joints (Hurmuzlu et al., 2004) and can be considered as an organized moving mechanical system that has many degrees of freedom (Aoi et al., 2007). The study of biped walking is important to design and manufacture more efficient artificial limbs for paraplegic people (Pournazhdi et al., 2011). Also, the biped robots or humanoids with the human-friendly appearance are suitable for care giving companions, navigation and assistance robots (Oda et al., 2012). The understanding and development of biped walking robots have been researched since the 1970s (Ono et al., 2001). During this period, biped walking robots have transformed into biped humanoid robots through the technological development (Kim et al., 2007).

One of the important goals of the research on humanoid robots is to make them coexist with human beings every day. For this, humanoids need to be able to behave "naturally" like human beings. This is certainly no exception to their bipedal locomotion. However, most currently existing biped robots do not walk naturally in that they bend their knees all the time during locomotion (Park et al., 2011).

Despite the fact that in most studies, modeling has been carried out *ignoring* the straight knee state of walking (Furusho et al., 1986; Cheng et al., 2000; Pettersson et al., 2001), in a few research works, some particular methods have been proposed in order to achieve a natural biped walking with straight knee (a detailed schematic of knee joint is depicted in Figure 1, when shank and thigh are aligned.).As a first attempt to accomplish the natural walking, it was proposed to consider a stretched knee. This was first introduced by Ogura et al. (2006). In the stretched knee technique, a singularity was introduced in the problem. In order to solve this problem, the idea was to avoid the singularity at the knee by settling the COG height lower so that the knee is always bent. In other words, by this technique, the knee joint is never straightened during the process of walking, which opposes the aim of natural walking (Ogura et al., 2006; Yoshida et al., 2012; Oda et al., 2012).

As a second attempt, a number of researchers have pointed out that the "stretched" state of knee should be considered as a constraint and not a singularity in the governing equations and do not avoid the stretched knee singularity. Noting that the body joints are the junctions of two or more system organs, the relative motion of some of these organs are restricted with respect to each other through the joint, which is referred to as self-impact joint. Considering joint self-impact phenomenon, as a natural property, in modeling of the body can exhibit a more realistic behavior of the system.

One way to consider the self-impact constraint is to assume a "stopper" at the knee joint, which was proposed in some research studies (Ono et al., 2000; Ono et al., 2001; Ono et al., 2004; Sangwan et al., 2004; Mukherjee et al., 2007; Huang et al., 2007; Hoshino et al., 2011; Zhihuan, 2011). The other way is to assume a "brake" at the knee joint, which was suggested by some other researchers (Ono et al., 2002; Ono et al., 2006). In the first technique, the main assumption is that the knee joint has a stopper that constrains the motion within the period where the knee angle is more than the hip angle and the stance leg links would be fully straight. The other interesting assumption is that this constraint takes place as a collision which is considered as a completely plastic impact. As a result, the modeling does not completely imitate natural walking (Ono et al., 2002; Ono et al., 2006). In the second technique, there was a bending angle held at the knee of the support leg. As a result, the biped model could walk faster than the fully straight support leg (stopper) model (Ono et al., 2000; Ono et al., 2001; Ono et al., 2004; Sangwan et al., 2004; Mukherjee et al. 2007; Huang et al., 2007; Hoshino et al., 2011; Zhihuan, 2011). Despite this assumption, the model included only an almost straight knee state, which does not exactly reproduce natural walking characteristics.

As the latest technique, Singh et al. (2008) modeled the impact at the lower (knee) joint of a self-impacting double pendulum using a spring–damper in combination with a logistic function in a computationally efficient manner.

When the self-impact constraint is imposed, the shank link of a leg cannot assume the rotation angles which are greater than that of the thigh link. Therefore, after the constraint is established (the constraint setting stage), the shank and thigh links may move together for some instants (the constrained motion stage) and natural walking is well imitated. In this paper, in order to use Singh's technique on a biped, the governing dynamical equations are modified due to the system switch from the free motion state to a constrained one which is represented by considering a torsional spring-damper system and two approximations of the Heaviside step function. These approximations are applied to the equations of motion, in order to account for continuity and physical consistency of the derived set of motion equations. On the other hand, designing a controller for this modified system will be a fundamental problem, due to its discontinuity and nonlinearity.

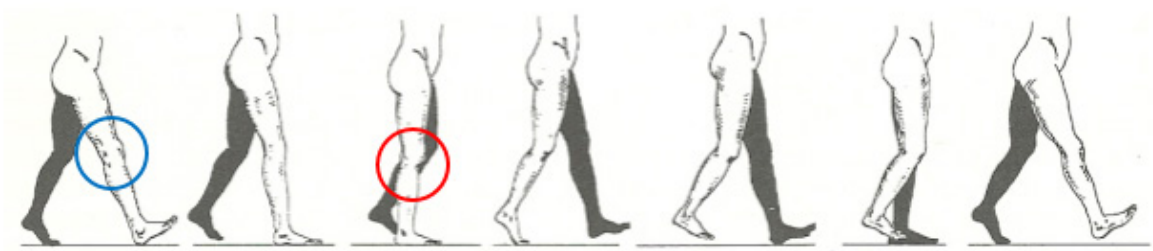


**Figure 1:** A detailed schematic of knee joint, when shank and thigh are aligned.

The control of bipedal robots considering self-impact constraint can be studied by two approaches. One of these approaches is that the energy which is dissipated from the system during the constraint establishment must be compensated in each gait cycle. Ono et al. obtained the dissipated energy due to joint self-impact stopper (Ono et al., 2000; 2001; 2004). In order to restore the dissi-

pated energy per cycle, they applied a torque to the hip joint model; this torque was determined by a simple proportional controller. This approach is appropriate for regulation purposes and not for tracking control of the (desired motion of the) constrained biped during the gait cycle. Also, in these studies, joint self-impact phenomenon was considered as a constraint in the governing equations using impulse and momentum approach, which is able to model the constraint setting stage, but unable to model the constrained motion stage.

The other approach is to use an advanced controller suitable for both regulation and tracking control problems of the biped including the self-impact constraint; we propose to utilize an adaptive neural network controller for this purpose. To carry out this objective, the available data of normal human gait will be considered as the desired trajectories of the hip and knee joints, which is anthropomorphic joint trajectory approach (Ounpuu, 1994; Kamen, 2001).

This paper is organized as follows: First, dynamic modeling of a biped considering joint self-impact constraint will be presented. Next, the control strategy for trajectory tracking control of the joint self-impact system will be described. The proposed control method, due to the nonlinear nature of this phenomenon, is Adaptive Neural Network approach. Finally, the simulation results are reported and discussed.

## 2 MATHEMATICAL DESCRIPTION OF DYNAMICAL MODELLING

As mentioned earlier, walking is one of the main gaits of human leg locomotion and is composed of two distinct phases: single support phase (SSP) and double support phase (DSP). SSP accounts for a much larger share in a walking gait cycle and that is why this phase has been the main focus of research study in this field.

The governing equations of the unconstrained system will be presented in section 2.1. At the completion of each gait cycle step, when the free end of the biped (swing leg) contacts with the ground, an instantaneous exchange of the biped support leg takes place, these are described in section 2.2 and section 2.3. We will model the joint self-impact phenomenon as a torsional spring-damper system and then present the governing equations of the constrained system presented, see section 2.4. In section 2.5, a unit step (Heaviside) function will be used in dynamical modeling of a self-impact biped to account for both the constraint setting and the constrained motion stages of the constraint; and to have them characterized in a unified manner. In the last section, dynamics of a self-impact biped will be modified by using another step function approximation for the system's physical consistency.

### 2.1 Governing equations of unconstrained biped in SSP

Figure 2 shows a schematics of an unconstrained biped. In this figure, $\theta_1$ and $\theta_5$ denote left and right knee rotation angles with regard to the vertical axis, respectively, $\theta_2$ and $\theta_4$ denote left and right hip rotation angles with regard to the vertical axis, respectively, and  is pelvis rotation angle. Dynamic equations of biped SSP based on Lagrange's method can be derived as follows:

$$M(\theta)\ddot{\theta} + C(\theta,\dot{\theta})\dot{\theta} + G(\theta) = \tau \tag{1}$$

where,

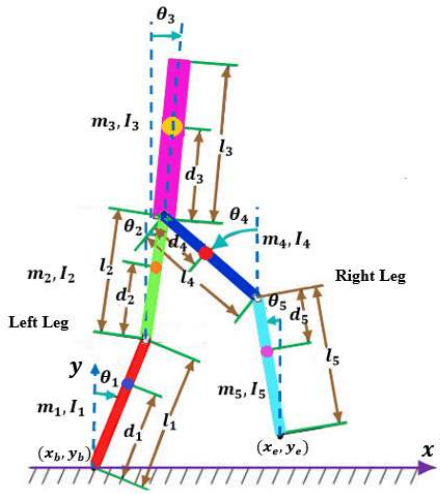



**Figure 2:** Schematics of an unconstrained biped.

$M = \left[M_{ij}\right] = p_{ij}\cos q_{ij}$ a $5\times 5$ positive definite and symmetric matrix of inertia.
$C = \left[C_{ij}\right] = p_{ij}h\dot{\theta}_j \sin q_{ij}$ a $5\times 5$ matrix related to the centrifugal and Coriolis terms.
$G = \left[G_i\right] = g_i \sin\theta_i$ a $5\times 1$ matrix of gravity terms.
$\tau$, a $5\times 1$ matrix of the applied external torques of motors.

and,

$$n_i = \begin{cases} 0 & i = 3,5 \\ \sum_{j=i+1}^{5} m_j l_j & \text{otherwise} \end{cases} \tag{2}$$

$$p_{ij} = p_{ji} = \begin{cases} I_i + m_i a_i^2 + n_i l_i & i = j \\ 0 & i = 3; j > i \\ m_j a_j l_i + n_j l_i & \text{otherwise} \end{cases} \tag{3}$$

$$q_{ij} = \begin{cases} \theta_i - \theta_j & i,j < 4 \quad \text{or} \quad i,j > 3 \quad i + j = 9 \\ 0 & i = j = 4 \quad \text{or} \quad i = j = 5 \\ \theta_i + \theta_j & \text{otherwise} \end{cases} \tag{4}$$

$$h = \begin{cases} -1 & i + j = 5 \quad \text{or} \quad i + j = 6 \\ 1 & \text{otherwise} \end{cases} \tag{5}$$

$$g_i = \begin{cases} -\left(m_i d_i + n_i\right) g & i < 4 \\ \left(m_i d_i + n_i\right) g & \text{otherwise} \end{cases} \tag{6}$$

## 2.2 Impact with ground phase

At the completion of each gait cycle step, when the free end of the biped (swing leg) contacts with the ground, an instantaneous exchange of the biped support leg takes place, while the other end

(the previous supporting leg) detaches immediately the ground. It is assumed that this process takes place in an infinitesimal time interval, equal to the previous impact duration. The angular velocity of each joint will be subjected to a jump discontinuity, which should be changed according to the velocities of the links just before and after the jump. The equation of this change is given by

$$\dot{\theta}^{+}_{impact} = \dot{\theta}^{-} + D^{-1}J^{T}\left[JD^{-1}J^{T}\right]^{-1}\left(-J\dot{\theta}^{-}\right) \tag{7}$$

where $\dot{\theta}^{+}_{impact}$ and $\dot{\theta}^{-}$ are vectors of generalized velocities immediately after and before the impact, respectively. Note that

$$\dot{\theta}^{+}_{impact} = \dot{\theta}^{-} + D^{-1}J^{T}\left[JD^{-1}J^{T}\right]^{-1}\left(-J\dot{\theta}^{-}\right) \tag{8}$$

where $\left(x_e, y_e\right)$ is the position of the tip of the swing leg is given by

$$\begin{cases} x_e = x_b + l_1\sin\theta_1 + l_2\sin\theta_2 + l_4\sin\theta_4 + l_5\sin\theta_5 \\ y_e = y_b + l_1\cos\theta_1 + l_2\cos\theta_2 - l_4\cos\theta_4 - l_5\cos\theta_5 \end{cases} \tag{9}$$

also, $D = \left[D_{ij}\right]$ is a $7\times 7$ inertia matrix and $J = \left[J_{ij}\right]$ is a $2\times 7$ Jacobian matrix, which are defined as below,

$$D_{ij} = \begin{cases} M_{ij} & i+j \le 10 \\ r_{ij}\cos\theta_i & i+j<11, j=6 \\ -r_{ij}u_i\sin\theta_i & i+j<12, j=7 \\ 0 & i+j=13 \\ r_{ij} & \text{others} \end{cases} \tag{10}$$

$$J_{ij} = \begin{cases} l_i\cos\theta_i & i=1,2,4,5\,,\ j=1 \\ l_i u_i\sin\theta_i & i=1,2,4,5\,,\ j=1 \\ 0 & i=3 \\ 1 & \text{others} \end{cases} \tag{11}$$

where,

$$r_{ij} = \begin{cases} m_i d_i + \sum_{\alpha=i+1}^{5} m_\alpha l_i & i=1,2,4 \\ m_i d_i & i=3,5 \\ \sum_{\beta=1}^{5} m_i & i=6,7 \end{cases} \tag{12}$$

$$u_i = \begin{cases} 1 & i=1,2,3,6 \\ -1 & i=4,5 \end{cases} \tag{13}$$

### 2.3 Phase exchange of the support end

As mentioned above, the roles of the swing and support leg exchanges. Therefore, in order to use the same set of motion equations of the SSP for both legs, the links numbering has to be relabeled. Such renumbering causes discontinuities in the angular displacements and velocities. This relabeling scheme is as follows:

$$\text{Link 1} \Leftrightarrow \text{Link 5}$$
$$\text{Link 2} \Leftrightarrow \text{Link 4}$$
$$\text{Link 3 does not change}$$

These lead to the following transformation equations, as the overall effect of the generalized coordinates immediately before and after the switch:

$$\begin{pmatrix} \theta^+ \\ \dot{\theta}^+ \end{pmatrix}_{\text{switch}} = \begin{pmatrix} T & 0_{5\times5} \\ 0_{5\times5} & T \end{pmatrix} \begin{pmatrix} \theta^- \\ \dot{\theta}^+_{\text{impact}} \end{pmatrix} \tag{14}$$

where,

$$\begin{pmatrix} \theta^- \\ \dot{\theta}^+_{\text{impact}} \end{pmatrix} \text{ and } \begin{pmatrix} \theta^+ \\ \dot{\theta}^+ \end{pmatrix}_{\text{switch}}$$

are the state space vectors specifying the coordinates and the velocities immediately before and after the switch, respectively, and  is the transformation matrix, which is defined as follows:

$$T = \begin{pmatrix} 0 & 0 & 0 & 0 & -1 \\ 0 & 0 & 0 & -1 & 0 \\ 0 & 0 & 1 & 0 & 0 \\ 0 & -1 & 0 & 0 & 0 \\ -1 & 0 & 0 & 0 & 0 \end{pmatrix} \tag{15}$$

### 2.4 Description of dynamical modelling of joint self-impact in a constrained biped

For an unconstrained biped, which is not a realistic model since there is no constraint in the knee joint, $\theta_1$ and $\theta_5$ may assume any values regardless of the amount of $\theta_2$ and $\theta_4$ rotation angle, respectively (see Figure 2). However, for genuine mammalian legs this assumption, i.e. no constraint on angles of rotation, is not valid and shank cannot assume the rotation angles which are greater than that of thigh. This discrepancy will be accounted for in system modeling by considering a self-impact constraint at the knee joints which will be activated when $\theta_1 \geq \theta_2$ and $\theta_5 \geq \theta_4$. In this situation, unlike the case for an unconstrained biped, we will have $\theta_1 = \theta_2$ and $\theta_5 = \theta_4$ for a constrained biped.

Ono et al. (2000); (2001); (2004); Huang et al. (2007) considered the joint self-impact constraint as a stopper. On the other hand, Singh et al. (2008); Chatterjee et al. (1995) used a spring and damper between two colliding members to model self-impact elastic and inelastic damper. The lat-

ter is a much better choice since it models both stages of the constraint setting and the constrained motion of the joint self-impact phenomenon. Figure 3 shows a self-impact biped as a model of a human leg while walking normally (Singh et al., 2008).

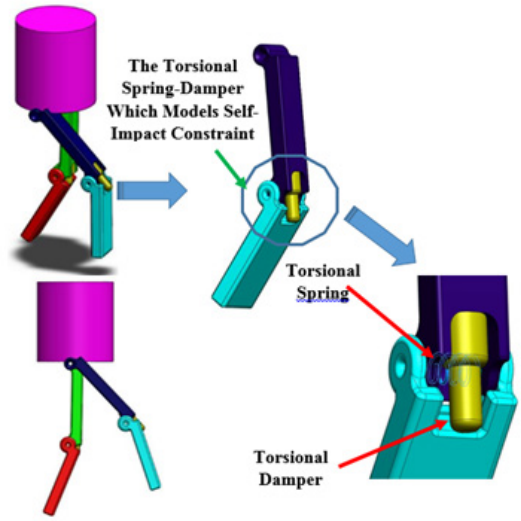



**Figure 3:** Schematics of a self-impact biped.

In Chatterjee et al. (1995) modelling, which is known as force-based method, the interaction force is described by a linear spring-damper element. The general form of this model is:

$$F_n = k\delta + c\dot{\delta} \tag{16}$$

where, $c$ and $k$ are the equivalent torsional damping and stiffness coefficients, respectively. And are rotation angle and angular velocity (Singh et al., 2008).

In addition, the joint self-impact phenomenon should be modeled by forces that are continually exerted between members in the time period of the activation of the constraint. Singh et al. (2008); Chatterjee et al. (1995), used Heaviside step function in their modeling to represent this constraint for its limited activation time. Therefore, dynamical equations for joint self-impact biped with torsional spring and damper as joint self-impact modeling will be modified as follows:

$$M(\theta)\ddot{\theta} + C(\theta,\dot{\theta})\dot{\theta} + G(\theta) + S(\theta,\dot{\theta}) = \tau \tag{17}$$

where, $S = \begin{bmatrix} s_1 & -s_1 & 0 & s_4 & -s_4 \end{bmatrix}^T$, a $5\times 1$ matrix of gravity terms; while the other terms are defined above.

$$s_i = \begin{cases} U\left(\theta_i - \theta_{i+1}\right)\left(k\left(\theta_{i+1} - \theta_i\right) + c\left(\dot{\theta}_{i+1} - \dot{\theta}_i\right)\right) & i = 1 \\ U\left(\theta_{i+1} - \theta_i\right)\left(k\left(\theta_i - \theta_{i+1}\right) + c\left(\dot{\theta}_i - \dot{\theta}_{i+1}\right)\right) & i = 4 \end{cases} \tag{18}$$

The terms $s_1$ and $s_4$ denotes the joint self-impact constraint in the left and right knees, respectively.

### 2.5 Approximation of heaviside step function for continuous modelling of joint self-impact constraint

In view of the fact that the step function creates discontinuities at the beginning of self-impact constraint, direct solution of equations with step function is not possible. To resolve this issue, Singh et al. (2008); Chatterjee et al. (1995) proposed to use the Fourier expansion (Harmonic) of the response and replaced it in the governing equations.

Since there is no harmonic forces in the joint self-impact biped, Fourier expansion can cause complex nonlinear equations and substantial reduction in the accuracy of the solution. The key point is that the Heaviside step function at the joint self-impact setting stage (when $\theta_1 = \theta_2$ and $\theta_5 = \theta_4$ for the left and right knees, respectively) is not differentiable. To solve the system of equations in a continuous domain, an approximation of the Heaviside function in the form of a continuous function is needed. The following is an example of a function that can be used for the approximating the Heaviside function Singh et al. (2008):

$$U\left(\theta_{j+1}-\theta_j\right) \approx \frac{1}{2}\left(1+\tanh\left[r\left(\theta_{j+1}-\theta_j\right)\right]\right) = \frac{1}{1+e^{-2r\left(\theta_{j+1}-\theta_j\right)}} \tag{19}$$

### 2.6 Physically consistent dynamical modelling of a constrained biped

Considering the spring and damper model for joint self-impact constraint equation (16), the joint self-impact constraint moment can be expressed as follows:

$$_{\text{left}}T_{ct}^{1} = k\left(\theta_1-\theta_2\right)+c\left(\dot{\theta}_1-\dot{\theta}_2\right) \tag{20}$$

$$_{\text{left}}T_{ct}^{2} = k\left(\theta_2-\theta_1\right)+c\left(\dot{\theta}_2-\dot{\theta}_1\right) \tag{21}$$

$$_{\text{right}}T_{ct}^{3} = k\left(\theta_5-\theta_4\right)+c\left(\dot{\theta}_5-\dot{\theta}_4\right) \tag{22}$$

$$_{\text{right}}T_{ct}^{4} = k\left(\theta_4-\theta_5\right)+c\left(\dot{\theta}_4-\dot{\theta}_5\right) \tag{23}$$

In general, for two rigid members undergoing self-impact constraint, the contact moments should always be positive. The condition $T_{ct}^{i} > 0$ is always satisfied in the above model, if the self-impact constraint at its setting stage is perfectly elastic. But since self-impact constraint is a passive phenomenon and there is some loss of energy involved at this stage, there can be a point where $T_{ct}^{i}$ crosses $0$ and becomes negative, which would imply local adhesion; however, each of the two members should be moving together (while the constraints are activated) or should be moving away from each other at the end of the constraint period of activation. Therefore, the "constraint moments" are in a direction that oppose the members' separation. To correct this physically inconsistent situation, we need to assure that each of the two members should separate completely from each other when $T_{ct}^{i} = 0$.

By replacing the above approximation in the previous equations and using approximation function for continuous improvement and correcting the physically inconsistency of the problem, the equations of motion of joint self-impact biped can be written as (Singh et al., 2008):

$$M(\theta)\ddot{\theta} + C(\theta,\dot{\theta})\dot{\theta} + G(\theta) + S(\theta,\dot{\theta}) = \tau \tag{24}$$

where the modified approximated $s_i$ is,

$$s_i = \begin{cases} \dfrac{\left(k\left(\theta_{i+1}-\theta_i\right)+c\left(\dot{\theta}_{i+1}-\dot{\theta}_i\right)\right)}{\left(1+e^{-2r\left(\theta_i-\theta_{i+1}\right)}\right)\left(1+e^{-2r\left(k\left(\theta_i-\theta_{i+1}\right)+c\left(\dot{\theta}_i-\dot{\theta}_{i+1}\right)\right)}\right)} & i=1 \\ \dfrac{\left(k\left(\theta_i-\theta_{i+1}\right)+c\left(\dot{\theta}_i-\dot{\theta}_{i+1}\right)\right)}{\left(1+e^{-2r\left(\theta_{i+1}-\theta_i\right)}\right)\left(1+e^{-2r\left(k\left(\theta_{i+1}-\theta_i\right)+c\left(\dot{\theta}_{i+1}-\dot{\theta}_i\right)\right)}\right)} & i=4 \end{cases} \tag{25}$$

## 3 TRACKING CONTROL OF THE JOINT SELF-IMPACT SYSTEM

To the best our knowledge, there has not been any publication on tracking control of any joint self-impact constrained biped system. The only research has been done by Bazargan-Lari et al. (2015), which deals with tracking control of a human swing leg. Also, there are a few articles on regulation problem of the constrained biped system by some researchers (Ono et al., 2000; 2001; 2002; 2004; 2006; Sangwan et al., 2004; Mukherjee et al., 2007; Huang et al., 2007; Hoshino et al., 2011; Zhihuan, 2011) and also by the authors, Bazargan-Lari et al. (2011).

For the tracking problem, the gait cycles of normal walking taken from anthropomorphic joint trajectories, Ounpuu (1994); Kamen (2001), should be assigned as the desired trajectories of the thigh, knee and pelvis joints of the constrained biped.

Due to complex nonlinear terms in the dynamic equations of self-impact biped, we propose to design a nonlinear intelligent controller by taking advantage of the Adaptive Neural Network control method, which neither requires the evaluation of the system inverse dynamical model nor the time-consuming training process.

There are a number of available control schemes in order to achieve accurate trajectory tracking and good control performance. One of the most intuitive schemes, which relies on the exact cancellation of the nonlinear dynamics of the manipulator system, is computed torque control method.

The main disadvantage of this method is that the exact dynamic model is required. For overcoming the problems of this method, adaptive control strategies have been developed and have attracted the interest of many researches, see for example: Craig et al. (1987); Slotine et al. (1987). An advantage of the adaptive control methods is the prior knowledge of unknown parameters is not a requirement.

To improve the performance of systems which have repetitive motions or operations, learning control schemes have been developed Arimoto (1990). A disadvantage of such a technique is that it is only applicable for operations which have repetition so that learning can take place.

There have been some developments in the use of neural networks for the control purposes, Miller et al. (1987); Miyamoto et al. (1988); Ozaki et al. (1991); Saad et al. (1994). In general, neural network control design has two steps. First the dynamic model of the system is approximated using neural network. Then, when this approximation, which is usually carried out off-line, is accurate enough, an appropriate control strategy there can be constructed. It is important to note that this approach does not have any built-in capability to deal with the changes in the system; therefore, incorporation of adaptive control becomes useful.

There have been some successful works by applying adaptive neural network (ANN) approach; they have been able to directly parameterize the control law by a suitable neural network, Sanner

et al. (1992); Tzirkel-Hancock et al. (1991). This has led to an overall closed-loop system with decent stability properties. Another advantage of this method is the evaluation of inverse dynamic model, as well as the time-consuming training process are not required anymore (Lewis et al., 1995; Ge et al., 1996). By assuming no prior knowledge about the system, the neural networks can be initialized in zero with no problems. Also, ANN controller is robust and easy to use for real time implementation.

### 3.1 Adaptive neural network control

In the field of control engineering, neural network is often used to approximate a given nonlinear function up to a small error tolerance. In this paper, Gaussian radial basis function (RBF) neural network is considered. It is a particular network architecture which uses / numbers of Gaussian function of the form (Wei et al., 2005):

$$a_i(y) = \exp\left(-\frac{\left(y-\mu_i\right)^T\left(y-\mu_i\right)}{\sigma^2}\right) \tag{26}$$

where $\mu_i \in R^n$ is the center vector and $\sigma^2 = R$ is the variance. As shown in Figure 4, Each Gaussian RBF network consists of three layers: the input layer, the hidden layer that contains the Gaussian function, and the output layer. The output of the Network $\hat{f}(W,y)$ can be given by:

$$\hat{f}(W,y) = W^T a(y) \tag{27}$$

where $a(y) = \begin{bmatrix} a_1(y) & a_2(y) & \cdots & a_l(y) \end{bmatrix}$ is the vector of basis function. Note that only the connections from the hidden layer to the output are weighted.

Gaussian RBF network has been quite successful in representing the complex nonlinear function. It has been proven that any continuous functions, not necessary infinitely smooth, can be uniformly approximated by a linear combination of Gaussians.

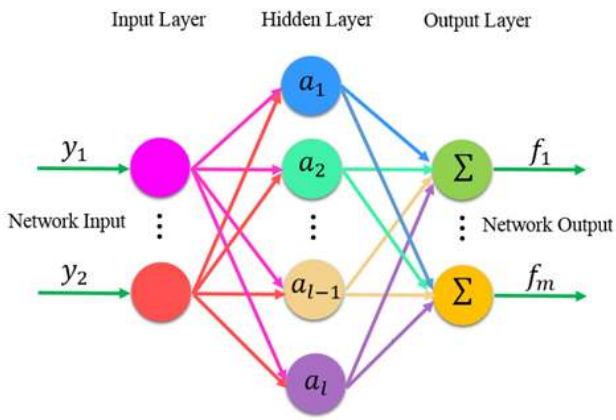



**Figure 4:** Gaussian radial basis function.

## 4 NEURAL NETWORK MODELING OF THE JOINT SELF-IMPACT SYSTEM

The dynamic equation of an n-degrees-of-freedom robot manipulator in joint space coordinates is given by:

$$M(q)\ddot{q} + C(q,\dot{q})\dot{q} + G(q) + \tau_f(q,\dot{q}) = \tau \tag{28}$$

where $q$, $\dot{q}$, $\ddot{q}$ the vectors $n \times 1$ are the joint angle, the $n \times 1$ joint angular velocity, and the $n \times 1$ joint angular acceleration, respectively; $M(q)$ is the symmetric positive definite inertia matrix; $C(q,\dot{q})\dot{q}$ is the vector of Coriolis and centrifugal torques satisfying $\dot{M}(q) - 2C(q,\dot{q})$ is a skew-symmetric matrix; $G(q)$ is the $n \times 1$ vector of gravitational torques; $\tau_f(q,\dot{q})$ is the $n \times 1$ vector of approximated joint self-impact constraint moment; $\tau$ is the $n \times 1$ vector of actuator joint torques; $f$ is the contact force.

It is observed that both $M(q)$ and $G(q)$ are functions of $q$ only; hence, static neural networks are sufficient to model them. Assume that $m_{kj}(q)$ and $g_k(q)$ can be modeled as:

$$m_{kj}(q) = \sum_l \theta_{kjl}\xi_{kjl}(q) + \varepsilon_{dkj}(q) = \theta_{kj}^T\xi_{kj}(q) + \varepsilon_{dkj}(q) \tag{29}$$

$$g_k(q) = \sum_l \beta_{kl}\eta_{kl}(q) + \varepsilon_{gk}(q) = \beta_k^T\eta_k(q) + \varepsilon_{gk}(q) \tag{30}$$

where $\theta_{kjl}, \beta_{kl} \in R$ are the weights of the neural networks, $\xi_{kj}(q), \eta_{kl}(q) \in R$ are the corresponding Gaussian basis functions with input vector $q$ and $\varepsilon_{dkj}(q), \varepsilon_{gk}(q) \in R$ are the modeling errors of $d_{kj}(q)$ and $g_k(q)$, respectively, and are assumed to be bounded. Whereas, for $C(q,\dot{q})$ a dynamic neural network of $q$ and $\dot{q}$ is needed to model it. Assume that $c_{kj}(q,\dot{q})$ can be modeled as:

$$c_{kj}(q,\dot{q}) = \sum_l \alpha_{kjl}\zeta_{kjl}(z) + \varepsilon_{ckj}(z) = \alpha_{kj}^T\zeta_{kj}(z) + \varepsilon_{ckj}(z) \tag{31}$$

where $z = \begin{bmatrix} q^T & \dot{q}^T \end{bmatrix}^T \in R$, $\alpha_{kjl} \in R$ is weight, is the corresponding Gaussian basis function with input vector $q$, and $\varepsilon_{ckj}$ is the modeling error of $c_{kj}(q,\dot{q})$, which is also assumed to be bounded. Therefore, equation (28) can be rewritten:

$$M(q)\ddot{q} + C(q,\dot{q})\dot{q} + G(q) + \tau_f(q,\dot{q}) = \tau$$

with:

$$m_{kj}(q) = \theta_{kj}^T\xi_{kj}(q) + \varepsilon_{dkj}(q) \tag{32}$$

$$c_{kj}(q,\dot{q}) = \alpha_{kj}^T\zeta_{kj}(z) + \varepsilon_{ckj}(z) \tag{33}$$

$$g_k(q) = \beta_k^T\eta_k(q) + \varepsilon_{gk}(q) \tag{34}$$

Using the GL matrix and its product operator introduced in section three, we can write $M(q)$ as:

$$M(q)=\left[\left\{\Theta\right\}^{T}\bullet\left\{\Xi\left(q\right)\right\}\right]+E_{M}\left(q\right)\ \Rightarrow M(q)=\begin{bmatrix}\theta_{11}^{T}\xi_{11}(q) & \theta_{12}^{T}\xi_{12}(q) & \cdots & \theta_{1n}^{T}\xi_{1n}(q)\\ \theta_{21}^{T}\xi_{21}(q) & \theta_{22}^{T}\xi_{22}(q) & \cdots & \theta_{2n}^{T}\xi_{2n}(q)\\ \vdots & \vdots & \vdots & \vdots\\ \theta_{n1}^{T}\xi_{n1}(q) & \theta_{n2}^{T}\xi_{n2}(q) & \cdots & \theta_{nn}^{T}\xi_{nn}(q)\end{bmatrix}+E_{M}(q) \quad (35)$$

$$C\left(q,\dot{q}\right)=\left[\left\{A\right\}^{T}\bullet\left\{Z\left(z\right)\right\}\right]+E_{C}\left(z\right)\ \Rightarrow C\left(q,\dot{q}\right)=\begin{bmatrix}\alpha_{11}^{T}\zeta_{11}(q,\dot{q}) & \alpha_{11}^{T}\zeta_{11}(q,\dot{q}) & \cdots & \alpha_{1n}^{T}\zeta_{1n}(q,\dot{q})\\ \alpha_{21}^{T}\zeta_{21}(q,\dot{q}) & \alpha_{22}^{T}\zeta_{22}(q,\dot{q}) & \cdots & \alpha_{2n}^{T}\zeta_{2n}(q,\dot{q})\\ \vdots & \vdots & \vdots & \vdots\\ \alpha_{n1}^{T}\zeta_{n1}(q,\dot{q}) & \alpha_{n2}^{T}\zeta_{n2}(q,\dot{q}) & \cdots & \alpha_{nn}^{T}\zeta_{nn}(q,\dot{q})\end{bmatrix}+E_{C}(q,\dot{q}) \quad (36)$$

$$G\left(q\right)=\left[\left\{B\right\}^{T}\bullet\left\{H\left(q\right)\right\}\right]+E_{G}\left(q\right)=\begin{bmatrix}\beta_{1}^{T}\eta_{1}\left(q\right)\\ \beta_{2}^{T}\eta_{2}\left(q\right)\\ \vdots\\ \beta_{n}^{T}\eta_{n}\left(q\right)\end{bmatrix}+E_{G}\left(q\right) \quad (37)$$

where $\left\{\Theta\right\}$, $\left\{\Xi\right\}$, $\left\{A\right\}$, $\left\{Z\left(z\right)\right\}$, $\left\{B\right\}$ and $\left\{H\left(q\right)\right\}$ are the GL matrices with their elements being $\theta_{kj}$, $\xi_{kj}\left(q\right)$, $\alpha_{kj}$, $\zeta_{kj}\left(z\right)$, $\beta_{k}$ and $\eta_{k}\left(q\right)$ respectively, as defined in appendix, and $E_{M}\left(q\right)\in R^{n\times n}$, $E_{C}\left(z\right)\in R^{n\times n}$ and $E_{G}\left(q\right)\in R^{n}$ are the matrices with their elements being the modeling errors $\varepsilon_{dkj}\left(q\right)$, $\varepsilon_{ckj}\left(z\right)$ and $\varepsilon_{gk}\left(q\right)$, respectively.

## 5 CONTROL SYSTEM DESIGN

Let $q_{d}(t)$ be the desired trajectory in the joint space and $\dot{q}_{d}(t)$, $\ddot{q}_{d}(t)$ be the desired velocity and acceleration. Define:

$$e(t)=q_{d}\left(t\right)-q\left(t\right) \quad (38)$$

$$\dot{q}_{r}\left(t\right)=\dot{q}_{d}\left(t\right)+\Lambda e\left(t\right) \quad (39)$$

$$r\left(t\right)=\dot{q}_{r}\left(t\right)-\dot{q}\left(t\right)=\dot{e}\left(t\right)+\Lambda e\left(t\right) \quad (40)$$

where $\Lambda$ is a positive definite matrix. According to the lemma, which is represent in the Wei et al. (2005), the stability of $e$ and $\dot{e}$ can be concluded by studying $r$.

Denote the estimate of $\left(\cdot\right)$ by $\left(\hat{\cdot}\right)$, and define $\left(\tilde{\cdot}\right)=\left(\cdot\right)-\left(\hat{\cdot}\right)$. Hence, $\left\{\hat{\Theta}\right\}$, $\left\{\hat{A}\right\}$ and $\left\{\hat{B}\right\}$ represent the estimates of the true parameter matrices $\left\{\Theta\right\}$, $\left\{A\right\}$ and $\left\{B\right\}$ respectively. According to Wei et al. (2005), the control law can be found as:

$$\tau=\left[\left\{\hat{\Theta}\right\}^{T}\bullet\left\{\Xi\left(q\right)\right\}\right]\ddot{q}_{r}+\left[\left\{\hat{A}\right\}^{T}\bullet\left\{Z\left(z\right)\right\}\right]\dot{q}_{r}+\left[\left\{\hat{B}\right\}\bullet\left\{H\left(q\right)\right\}\right]+Kr+k_{s}\mathrm{sgn}\left(r\right) \quad (41)$$

where $K\in R^{n\times n}$ and $k_{s}>\left\|E\right\|$, with $E=E_{M}\left(q\right)\ddot{q}_{r}+E_{C}\left(z\right)\dot{q}_{r}+E_{G}\left(q\right)+\tau_{f}\left(q,\dot{q}\right)$. The first three terms of the control law are the model-based control, whereas the $Kr$ term gives the proportional derivative (PD) type of control. Note that the PD control is effectively introduced to the control law through the definition of $r$ given in equation (40). The last term in the control law is added to

suppress the modeling errors of the neural networks. The parameters in the control law are updated by:

$$\dot{\hat{\theta}} = \Gamma \bullet \left\{ \xi_k \left( q \right) \right\} \ddot{q}_r r_k \tag{42}$$

$$\dot{\hat{\alpha}} = Q_k \bullet \left\{ \zeta_k \left( z \right) \right\} \dot{q}_r r_k \tag{43}$$

$$\dot{\hat{\alpha}} = Q_k \bullet \left\{ \zeta_k \left( z \right) \right\} \dot{q}_r r_k \tag{44}$$

where $\Gamma_k$, $Q_k$ and $N_k$ are positive definite and symmetric; and $\hat{\theta}$, $\hat{\alpha}$ are the column vectors with their elements being $\hat{\theta}_{kj}$ and $\hat{\alpha}_{kj}$, respectively.

## 6 SIMULATION RESULTS

In this section the results of simulation of tracking control of a self-impact biped will be presented. The simulation is performed via a commercial software and involves complex nonlinear terms in the dynamical governing equations which provide natural bipedal walking. Walking control of biped robots is classically performed via prescribed reference trajectory tracking. These trajectories can be of different types: (i) anthropomorphic joint trajectories (Vukobratovic et al., 1990), which is used in this paper, derived from human walking, (ii) torque trajectories (Goswami et al., 1996); Pratt et al., 1998) or (iii) optimal trajectories computed off-line (Chevallereau et al., 1997; Chessé et al., 2001).

Table 1 shows the anthropometric dimensions and masses which match the parameters presented in reference Kamen (2001). Also, the desired trajectories of the hip, knee and pelvis joints of the self-impact biped are taken from the available normal gait cycle data (Ounpuu, 1994; Kamen, 2001).

| Parameter | Description | Value |
|---|---|---|
| $m_1, m_5$ | Masses of shank links | 0.1 kg |
| $m_3$ | Mass of trunk link | 0.1 kg |
| $m_2, m_4$ | Masses of thigh links | 0.1 kg |
| $l_1, l_5$ | Lengths of shank links | 0.1 kg |
| $l_3$ | Length of trunk link | 0.1 kg |
| $l_2, l_4$ | Lengths of thigh links | 0.1 kg |
| $c$ | Damping coefficient | 2.4 N.s/rad |
| $k$ | Stiffness coefficient | 42 N/rad |
| $r$ | Accuracy of the approximating function | 10E5 |
| $n_m$ | Number of the static neural network nodes | 12 Nodes |
| $n_c$ | Number of the dynamic neural network nodes | 24 Nodes |
| $n_a$ | Number of the static neural network nodes | 12 Nodes |
| $\mu$ | The center Vector of the Gaussian RBF | 0 |
| $\sigma^2$ | The Variance of the Gaussian RBF | 10 |

**Table 1:** The parameters used to simulate the locomotion of a self-impact biped.

### 6.1 The gait cycles of normal walking taken as the desired joint angles of the hip, knee and pelvis joints

The desired trajectories of the left and right hip and knee joints of a typical human (Ounpuu, 1994; Kamen, 2001) are presented in Figure 5a and Figure 6a, respectively. In these figures, the periods in which the self-impact phenomenon occur are highlighted by **A** and **B** letters and colored in green and blue for both phases of stance and swing, respectively and separately (Figures 5b, 5c, 6b, 6c). The desired trajectory of the pelvis joint is also depicted in Figure 7. In order to provide the desired angular velocities of the hip, knee and pelvis joints, since there are no reported experimental data for them, one efficient way would be to take the numerical time derivative of the curves of Figures 5a, 6a, 7. The obtained desired angular velocities of the hip, knee and pelvis joints can be seen in Figure 8.

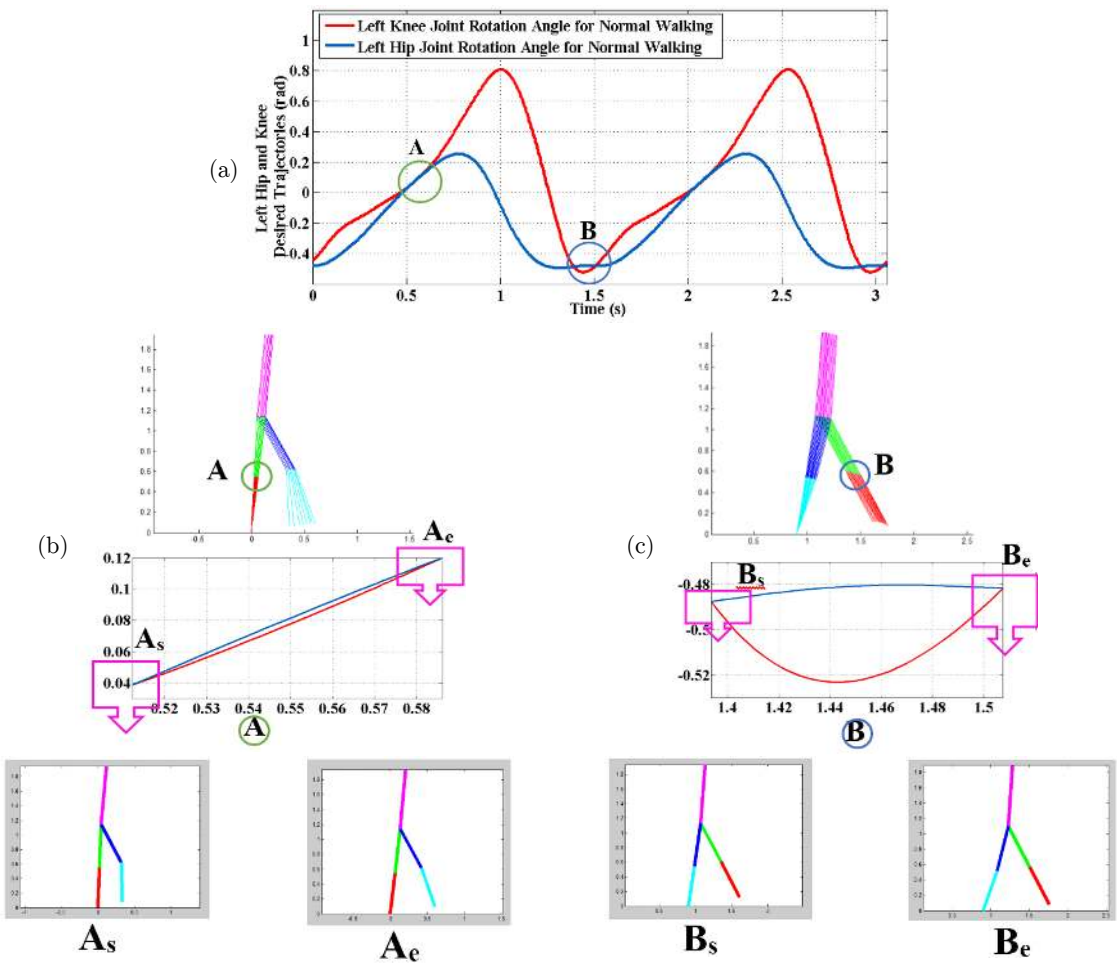



**Figure 5:** (a) A typical human's left hip and knee normal gait cycles Ounpuu, (1994).
(b) The period of the self-impact constraint activation in the stance phase.
(c) The period of the self-impact constraint activation in the swing phase.
(d) The beginning of the activation period, the stance phase.
(e) The end of the activation period, the stance phase.
(f) The beginning of the activation period, the swing phase.
(g) The end of the activation period, the swing phase.

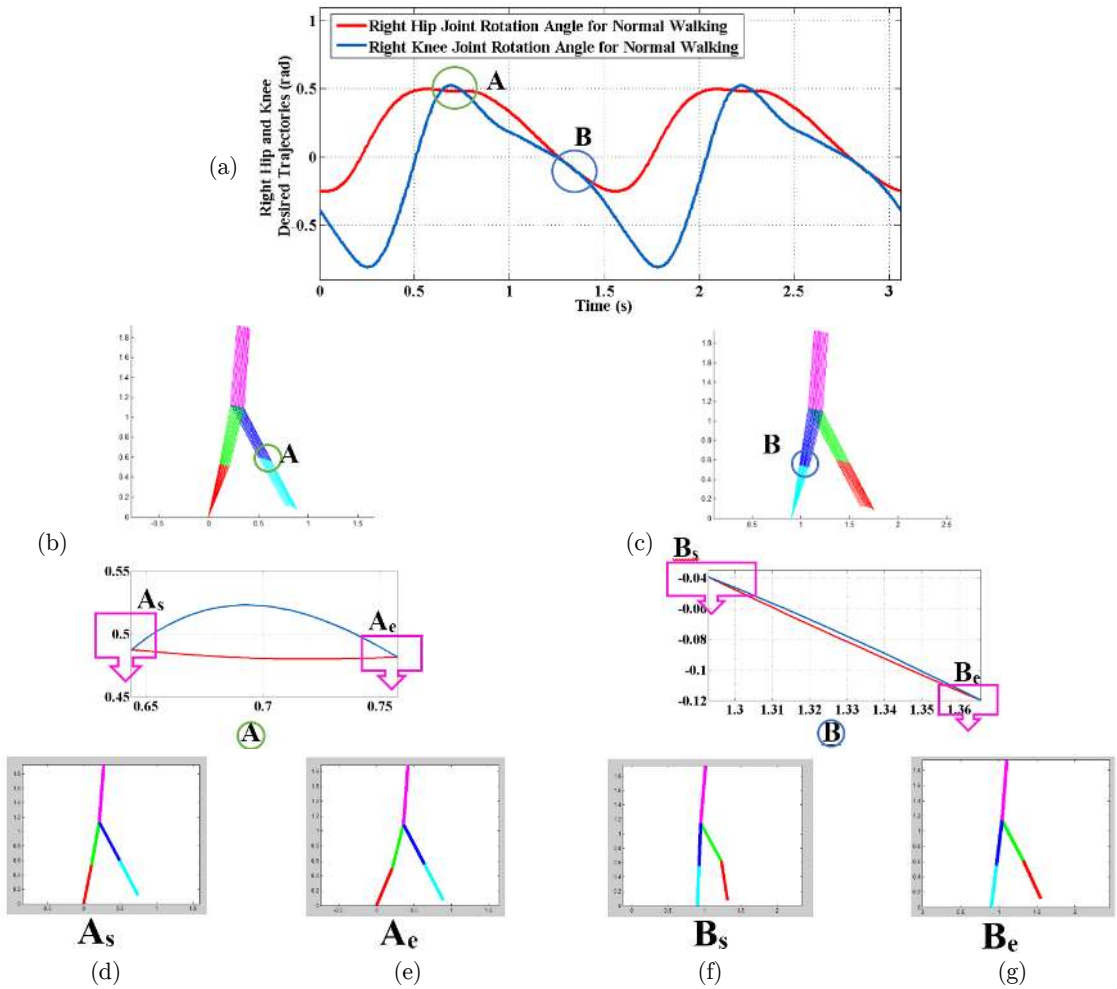



**Figure 6:** (a) A typical human's Right hip and knee normal gait cycles Ounpuu (1994).
(b) The period of the self-impact constraint activation in the swing phase.
(c) The period of the self-impact constraint activation in the stance phase.
(d) The beginning of the activation period, the swing phase.
(e) The end of the activation period, the swing phase.
(f) The beginning of the activation period, the stance phase.
(g) The end of the activation period, the stance phase.

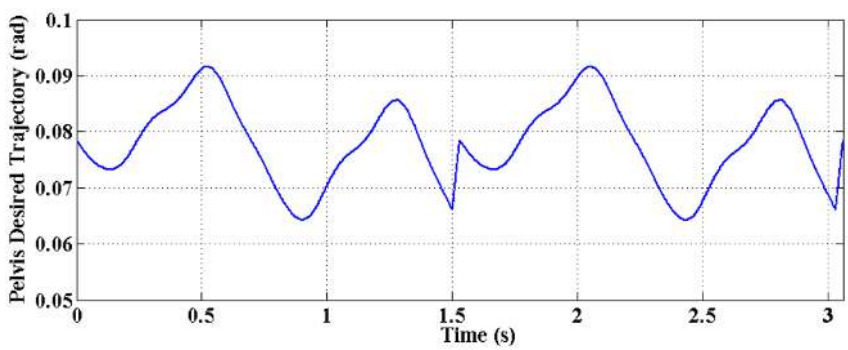



**Figure 7:** Human's pelvis normal gait cycles, Ounpuu (1994).

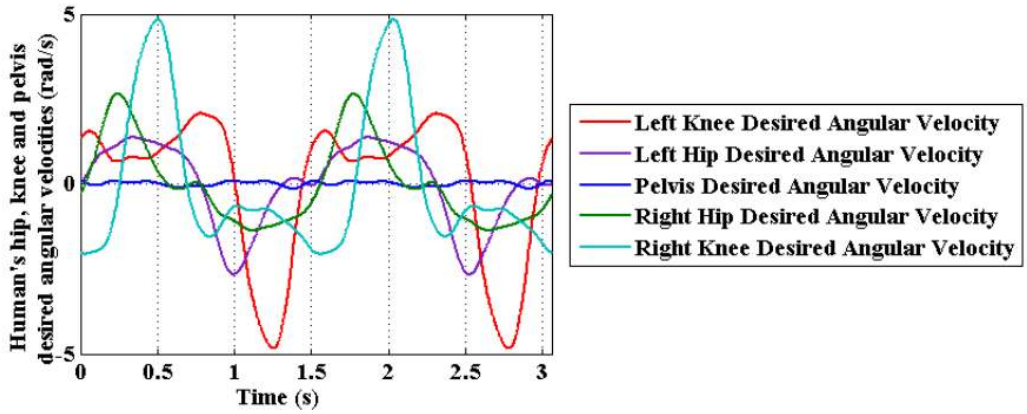



**Figure 8:** A typical human's hip, knee and pelvis desired angular velocities.

### 6.2 The block diagram of the proposed controller

In this article, adaptive neural network method is proposed to be used for the trajectory tracking of a self-impact constrained biped. The structure of the controller is shown in Figure 9.

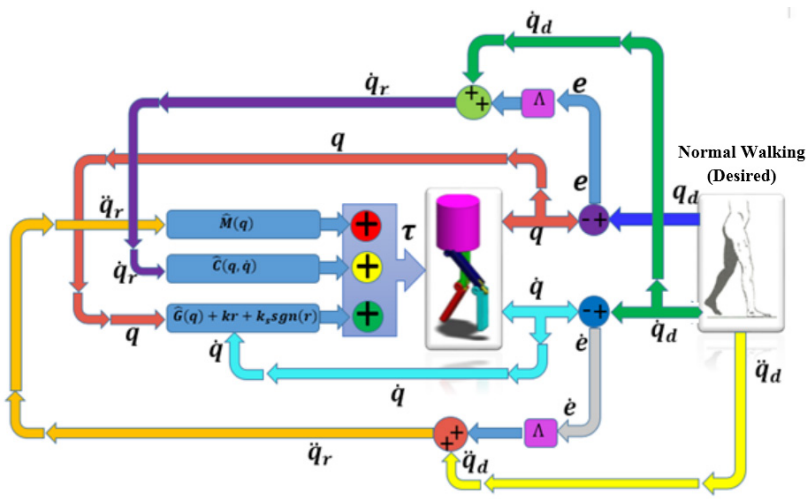



**Figure 9:** The block diagram of the adaptive neural network controller.

### 6.3 The simulation results

The purpose of the present study is to simulate the tracking control of a self-impact biped. Figures 10a, 11a, 12, 13a, 14a show the desired and tracked trajectories of the left knee, left hip, right hip, right knee and pelvis joints, respectively; as it can be seen, all the tracked and the corresponding desired trajectories remarkably match each other. The time histories of the errors between the tracked and the corresponding desired angles for these joints are shown in Figure 15a; the maximum errors for the activation periods are listed in Table 2. Also, the time histories of the errors between the tracked and the corresponding desired angular velocities for these joints are shown in Figure 16a; the maximum errors for the activation periods are listed in Table 3. Finally, Figure 17a shows the time histories of the applied torques for the same joints.

| Joints | | Period of self-impact | | Maximum error | |
|---|---|---|---|---|---|
| | | Stance | Swing | Stance | Swing |
| Left | Hip | 0.5123-0.5861 | 1.3937-1.5075 | $0.8\text{x}10^{-5}$ | $1.3\text{x}10^{-3}$ |
| | Knee | 0.5123-0.5861 | 1.3937-1.5075 | $1.1\text{x}10^{-5}$ | $7.5\text{x}10^{-4}$ |
| Right | Hip | 1.2928-1.3658 | 0.6436-0.7575 | $5.5\text{x}10^{-5}$ | $1.1\text{x}10^{-3}$ |
| | Knee | 1.2928-1.3658 | 0.6436-0.7575 | $5.3\text{x}10^{-4}$ | $2.1\text{x}10^{-4}$ |
| Pelvis | | 0.5123-0.5861 | 1.3937-1.5075 | $0.4\text{x}10^{-5}$ | $0.5\text{x}10^{-4}$ |
| | | 1.2928-1.3658 | 0.6436-0.7575 | $1.2\text{x}10^{-4}$ | $0.25\text{x}10^{-4}$ |

**Table 2:** The periods of self-impact constraint activation and the corresponding errors of the biped joints.

| Joints | | Period of self-impact | | Maximum error | |
|---|---|---|---|---|---|
| | | Stance | Swing | Stance | Swing |
| Left | Hip | 0.5123-0.5861 | 1.3937-1.5075 | $1.3\text{x}10^{-3}$ | $6.5\text{x}10^{-3}$ |
| | Knee | 0.5123-0.5861 | 1.3937-1.5075 | $1.5\text{x}10^{-3}$ | $1.2\text{x}10^{-2}$ |
| Right | Hip | 1.2928-1.3658 | 0.6436-0.7575 | $1.7\text{x}10^{-2}$ | $0.8\text{x}10^{-2}$ |
| | Knee | 1.2928-1.3658 | 0.6436-0.7575 | $1.8\text{x}10^{-2}$ | $1.5\text{x}10^{-2}$ |
| Pelvis | | 0.5123-0.5861 | 1.3937-1.5075 | $0.4\text{x}10^{-3}$ | $0.6\text{x}10^{-3}$ |
| | | 1.2928-1.3658 | 0.6436-0.7575 | $2.5\text{x}10^{-3}$ | $0.4\text{x}10^{-3}$ |

**Table 3:** The periods of self-impact constraint activation and the corresponding errors of the biped joints angular velocity errors.

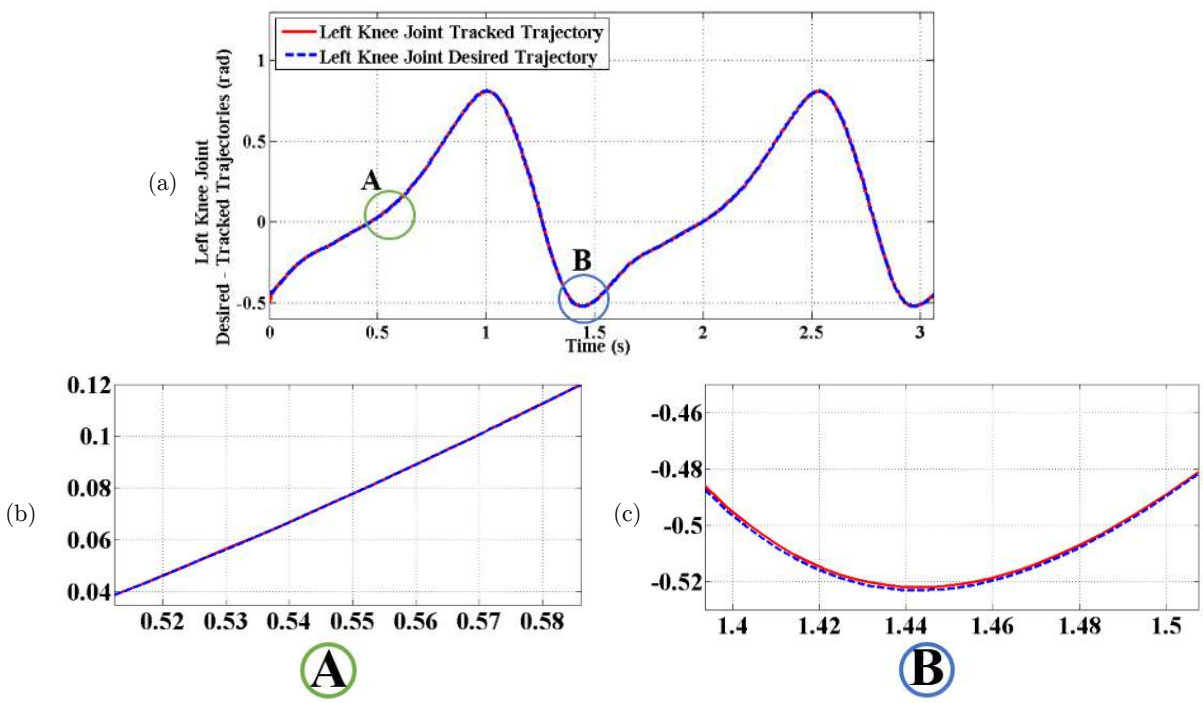



**Figure 10:** (a) The desired and tracked trajectories of left knee joint of a self-impact biped for two gait cycles.
(b) The period of the self-impact constraint activation in the stance phase.
(c) The period of the self-impact constraint activation in the swing phase.

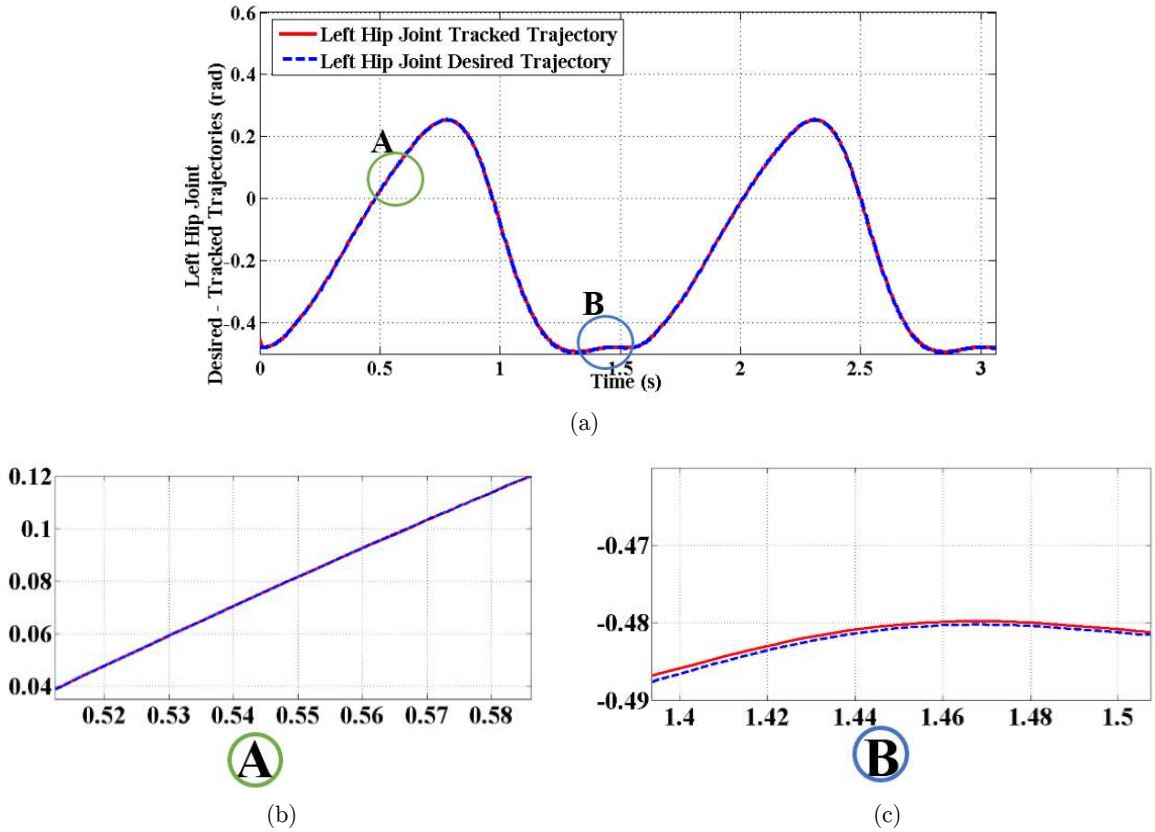



**Figure 11:** (a) The desired and tracked trajectories of Left hip joint of a self-impact biped for two gait cycles
(b) The period of the self-impact constraint activation in the stance phase
(c) The period of the self-impact constraint activation in the swing phase

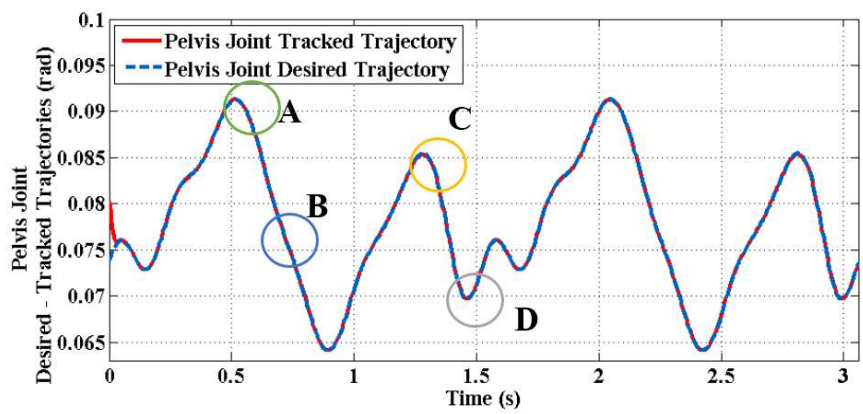



**Figure 12:** Human's pelvis normal gait cycles, Ounpuu (1994).

Figures 16a, 17a show, respectively, sudden changes in the joint angular velocity errors and the applied motor torques when the self-impact constraint is activated. Despite these sudden changes, the controller makes the biped follow the joint desired trajectories very closely with insignificant errors and feasible torques.

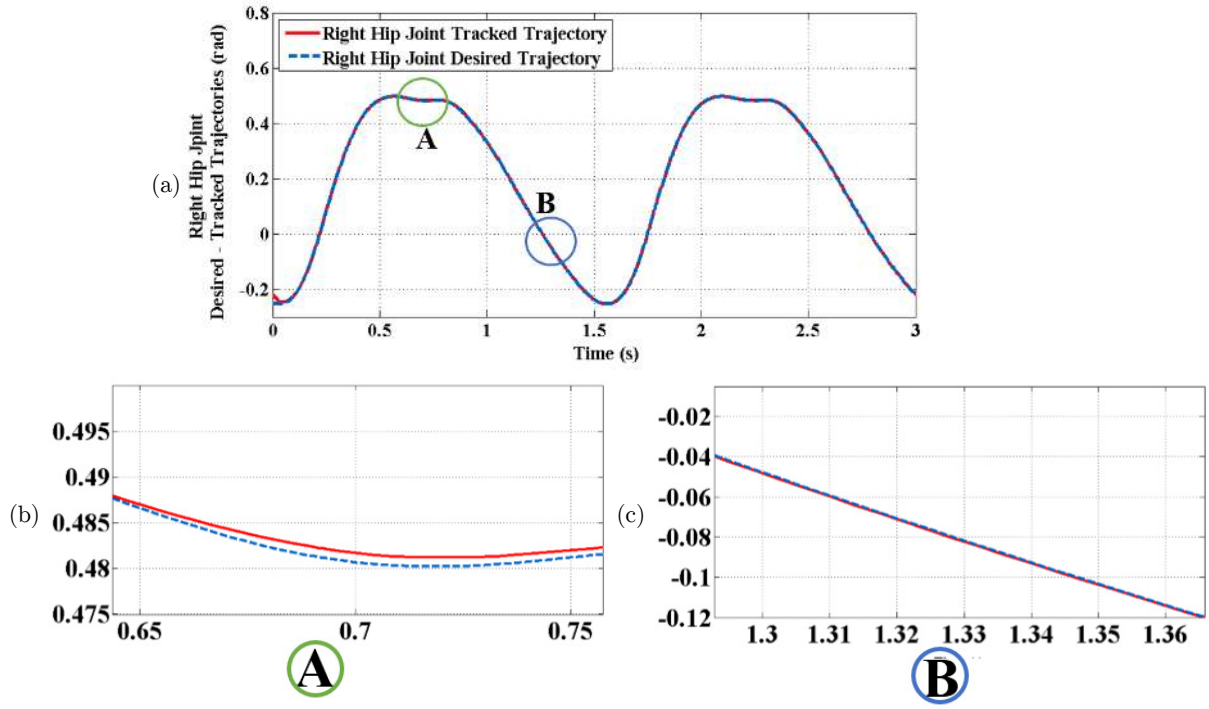



**Figure 13:** (a) The desired and tracked trajectories of Right hip joint of a self-impact biped for two gait cycles.
(b) The period of the self-impact constraint activation in the swing phase.
(c) The period of the self-impact constraint activation in the stance phase.

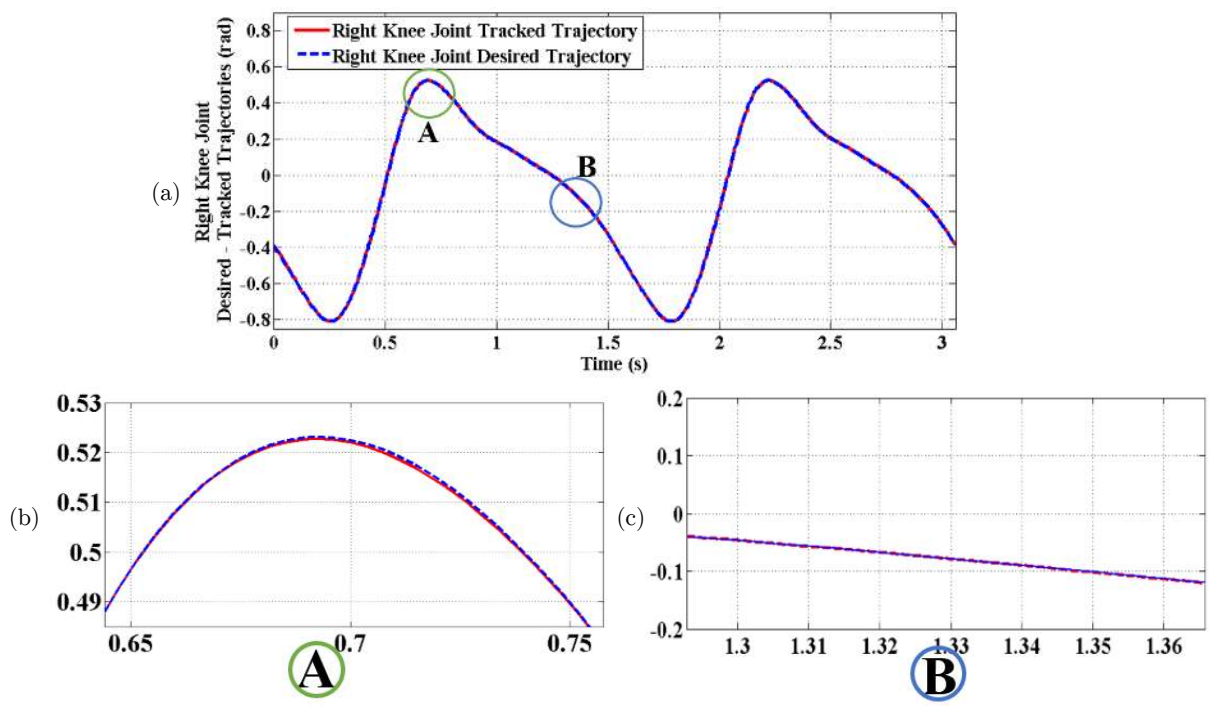
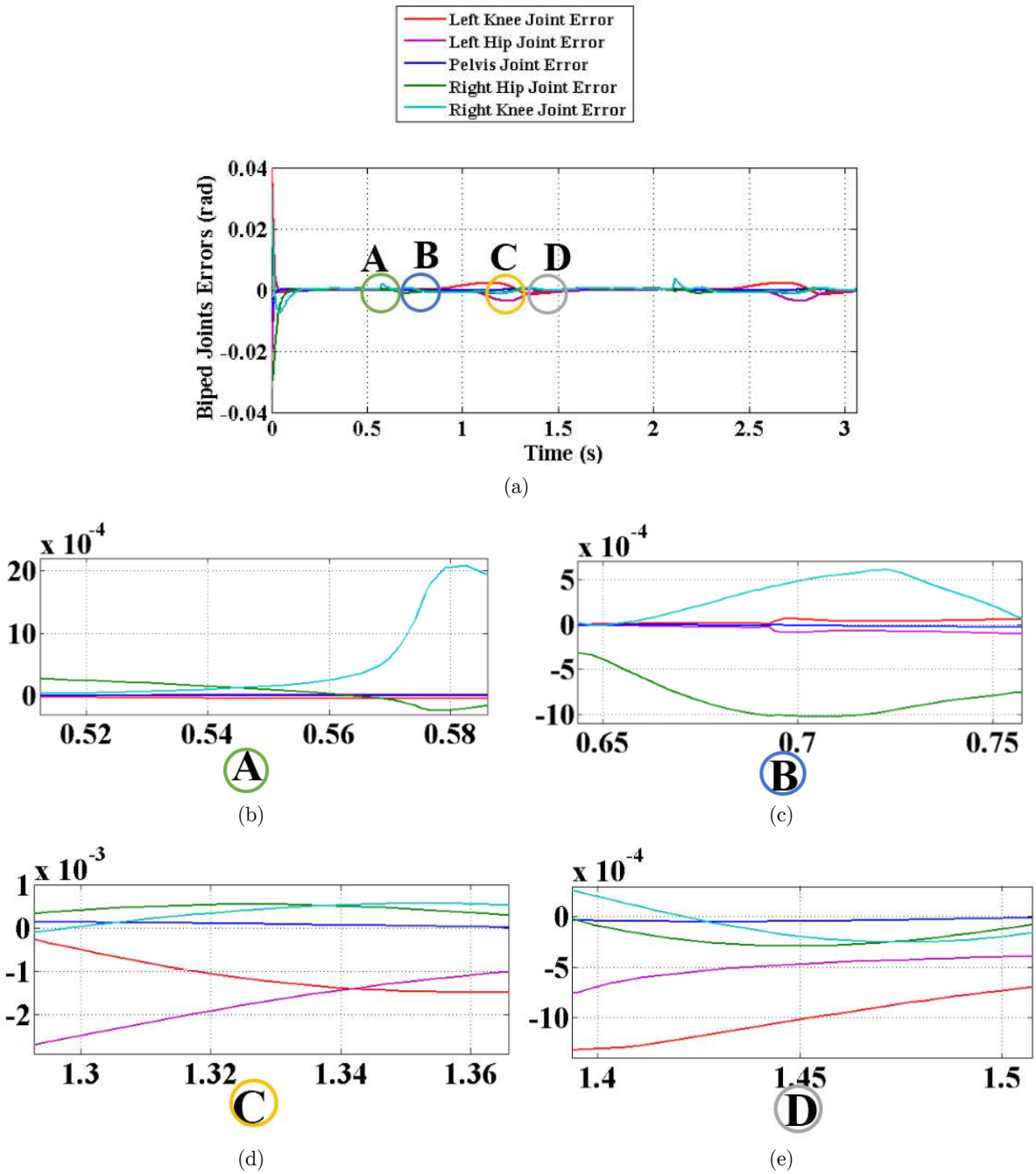



**Figure 14:** (a) The desired and tracked trajectories of Right knee joint of a self-impact biped for two gait cycles.
(b) The period of the self-impact constraint activation in the swing phase.
(c) The period of the self-impact constraint activation in the stance phase.




(a)

(b)

(c)

(d)

(e)

**Figure 15:** (a) The time histories of the errors between the tracked and the corresponding desired angles for the joints of a self-impact biped.
(b) The period of the self-impact constraint activation in the left leg stance phase.
(c) The period of the self-impact constraint activation in the right leg swing phase.
(d) The period of the self-impact constraint activation in the left leg swing phase.
(e) The period of the self-impact constraint activation in the right leg stance phase.

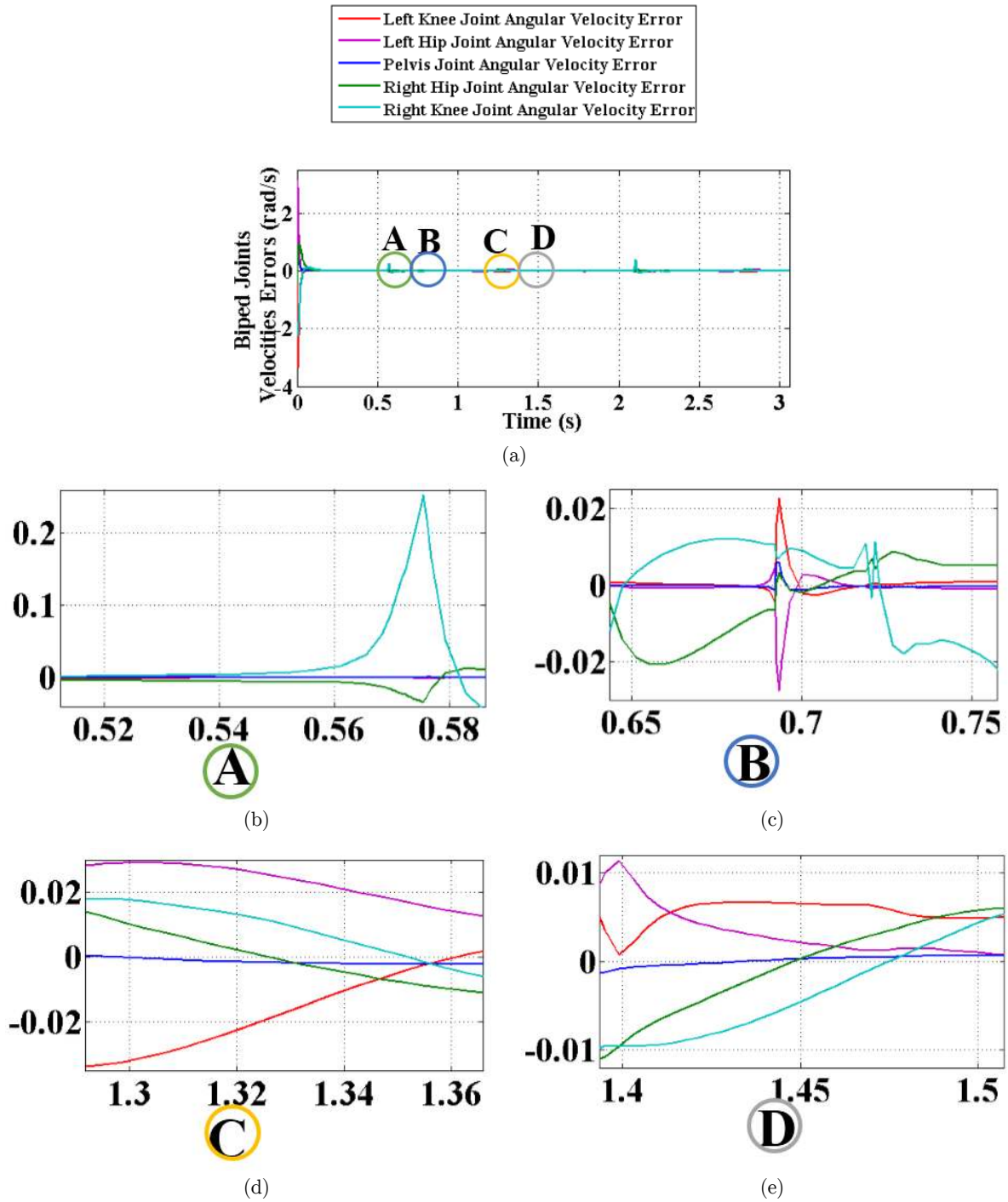



**Figure 16:** (a) Time history of the constrained biped joints angular velocity errors.
(b) The period of the self-impact constraint activation in the left leg stance phase.
(c) The period of the self-impact constraint activation in the right leg swing phase.
(d) The period of the self-impact constraint activation in the left leg swing phase.
(e) The period of the self-impact constraint activation in the right leg stance phase.

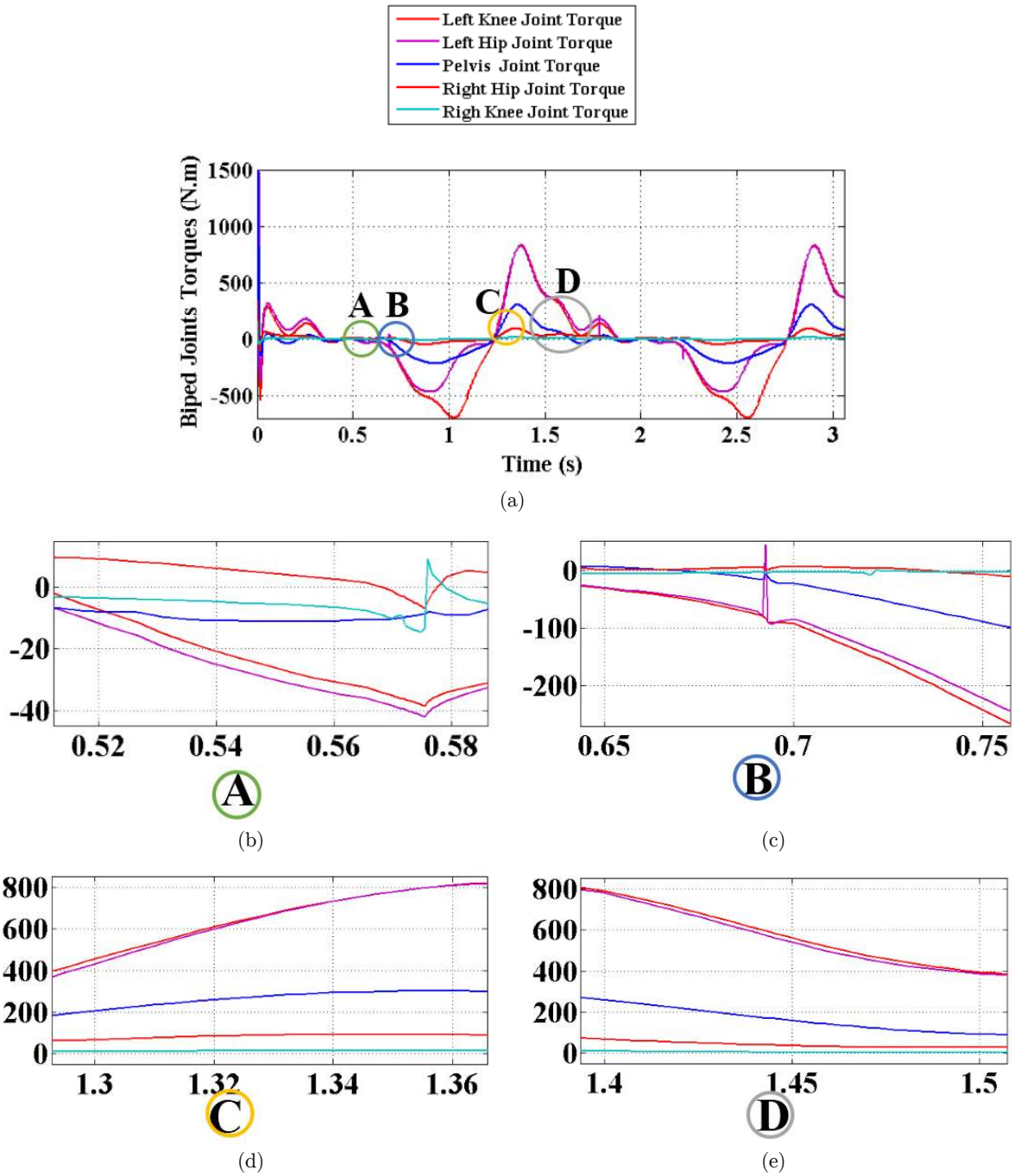



**Figure 17:** (a) Time histories of the constrained biped joint torques.
(b) The period of the self-impact constraint activation in the left leg stance phase.
(c) The period of the self-impact constraint activation in the right leg swing phase.
(d) The period of the self-impact constraint activation in the left leg swing phase.
(e) The period of the self-impact constraint activation in the right leg stance phase.

## 7 CONCLUSIONS

The objective of this paper was to present a model-based control method for trajectory tracking of a constrained biped in normal human walking, by considering the joint self-impact constraint. To achieve this objective, first, the dynamical equations of motion of an unconstrained biped were taken, developed and then modified to consider the joint self-impact constraint at the knee joint. Two approximations of the Heaviside step function were applied to the equations of motion, in order to account for continuity and physical consistency of the derived set of motion equations.

To control this complicated system, the available anthropometric normal gait cycle data were taken to generate the desired trajectories of the thigh and knee joints of a self-impact biped. Due to the existence of complex nonlinear terms in the dynamical governing equations of the self-impact biped, the authors proposed to design a nonlinear intelligent controller by taking advantage of the adaptive neural network control method, which neither requires the evaluation of inverse dynamical model nor the time-consuming training process.

According to the simulation results, the anthropometric normal gait cycle data of the rotation angles of the hip, knee and pelvis joints of both legs were well followed by the simulated constrained biped. The joint self-impact constraint was activated in two occasions for each leg, one corresponding to the swing phase period and the other one to the stance phase period. In these periods, even in the presence of sudden changes in the hip and knee angular velocities during the constraint activation stages, the hip, knee and pelvis joints tracked their desired values of the rotation angles with acceptable errors. Also, comparable results were obtained for the joint angular velocities. The results showed that the system was well controlled with insignificant errors and in a proper time period by feasible controlled applied torques, despite the existence of complex nonlinear terms in the dynamical governing equations of the system.

### References

Aoi, S., Tsuchiya, K., (2007). Self-stability of a simple walking model driven by a rhythmic signal. Nonlinear Dynamics 48(1-2): 1-16.

Arimoto, S., (1990). Learning control theory for robotic motion. International Journal of Adaptive Control and Signal Processing 4(6): 543-564.

Azevedo, C., Poignet, P., Espiau, B., (2004). Artificial locomotion control: from human to robots. Robotics and Autonomous Systems 47(4): 203-223.

Bazargan-Lari, Y., Gholipour, A., Eghtesad, M., Nouri, M., Sayadkooh, A., (2011, December). Dynamics and control of locomotion of one leg walking as self-impact double pendulum. In Control, Instrumentation and Automation (ICCIA), 2011 2nd International Conference on (pp. 201-206). IEEE.

Bazargan-Lari, Y., Eghtesad, M., Khoogar, A., Mohammad-Zadeh, A., (2015). Tracking control of a human swing leg considering self-impact joint constraint by feedback linearization method. Journal of Control Engineering and Applied Informatics 17(1): 99-110.

Chatterjee, S., Mallik, A.K., Ghosh, A., (1995). On impact dampers for non-linear vibrating systems. Journal of Sound and Vibration 187(3): 403-420.

Cheng, M.Y., Lin, C.S., (2000). Dynamic biped robot locomotion on less structured surfaces. Robotica 18(02): 163-170.

Chessé, S., Bessonnet, G., (2001). Optimal dynamics of constrained multibody systems. Application to bipedal walking synthesis. In Robotics and Automation, 2001. Proceedings 2001 ICRA. IEEE International Conference on (Vol. 3, pp. 2499-2505). IEEE.

Chevallereau, C., Formal'Sky, A., Perrin, B., (1997, April). Control of a walking robot with feet following a reference trajectory derived from ballistic motion. In Robotics and Automation, 1997. Proceedings., 1997 IEEE International Conference on (Vol. 2, pp. 1094-1099). IEEE.

Craig, J.J., Hsu, P., Sastry, S.S., (1987). Adaptive control of mechanical manipulators. The International Journal of Robotics Research 6(2): 16-28.

Furusho, J., Masubuchi, M., (1986). Control of a dynamical biped locomotion system for steady walking. Journal of Dynamic Systems, Measurement, and Control 108(2): 111-118.

Ge, S.S., Hang, C.C., (1996). Direct adaptive neural network control of robots. International journal of systems science 27(6): 533-542.

Ge, S.S., (1996). Robust adaptive NN feedback linearization control of nonlinear systems. International journal of systems science 27(12): 1327-1338.

Goswami, A., Espiau, B., Keramane, A., (1996, April). Limit cycles and their stability in a passive bipedal gait. In Robotics and Automation, 1996. Proceedings., 1996 IEEE International Conference on (Vol. 1, pp. 246-251). IEEE.

Hoshino, Y., Fu, C., Chen, K., (2011, August). A passive walking strategy for a biped robot with a large mass torso by a spring and a damper. In Mechatronics and Automation (ICMA), 2011 International Conference on (pp. 1269-1274). IEEE.

Huang, Q., Ono, K., (2007). Energy-efficient walking for biped robot using self-excited mechanism and optimal trajectory planning. Humanoid Robots: New Developments, Chapter 19.

Hurmuzlu, Y., Génot, F., Brogliato, B., (2004). Modeling, stability and control of biped robots—a general framework. Automatica 40(10): 1647-1664.

Kamen, G., (Ed.). (2001). Foundations of exercise science. Introduction to biomechanics, Lippincott Williams & Wilkins.

Kim, J.Y., Park, I.W., Oh, J.H., (2007). Walking control algorithm of biped humanoid robot on uneven and inclined floor. Journal of Intelligent and Robotic Systems 48(4): 457-484.

Lewis, F.L., Liu, K., Yesildirek, A., (1995). Neural net robot controller with guaranteed tracking performance. Neural Networks, IEEE Transactions on 6(3): 703-715.

Miller, W.T., Glanz, F.H., Kraft, L.G., (1987). Application of a general learning algorithm to the control of robotic manipulators. The International Journal of Robotics Research 6(2): 84-98.

Miyamoto, H., Kawato, M., Setoyama, T., Suzuki, R., (1988). Feedback-error-learning neural network for trajectory control of a robotic manipulator. Neural Networks 1(3): 251-265.

Mukherjee, S., Sangwan, V., Taneja, A., Seth, B., (2007). Stability of an underactuated bipedal gait. Biosystems 90(2): 582-589.

Oda, N., Yanada, O., (2012, October). Motion controller design of biped robot for human-like walking with stretched knee. In IECON 2012-38th Annual Conference on IEEE Industrial Electronics Society (pp. 5434-5439). IEEE.

Ogura, Y., Shimomura, K., Kondo, H., Morishima, A., Okubo, T., Momoki, S., Takanishi, A., (2006, October). Human-like walking with knee stretched, heel-contact and toe-off motion by a humanoid robot. In Intelligent Robots and Systems, 2006 IEEE/RSJ International Conference on (pp. 3976-3981). IEEE.

Ono, K., Takahashi, R., Imadu, A., Shimada, T., (2000). Self-excitation control for biped walking mechanism. In Intelligent Robots and Systems, 2000. (IROS 2000). Proceedings. 2000 IEEE/RSJ International Conference on (Vol. 2, pp. 1143-1148). IEEE.

Ono, K., Takahashi, R., Shimada, T., (2001). Self-excited walking of a biped mechanism. The International Journal of Robotics Research 20(12): 953-966.

Ono, K., Yao, X., Hou, J., (2002, August). Simulation study on fast biped walking based on self-excitation. In SICE 2002. Proceedings of the 41st SICE Annual Conference (Vol. 4, pp. 2553-2558). IEEE.

Ono, K., Furuichi, T., Takahashi, R., (2004). Self-excited walking of a biped mechanism with feet. The International Journal of Robotics Research 23(1): 55-68.

Ono, K., Yao, X., (2006). Simulation study of self-excited walking of a biped mechanism with bent knee. In Adaptive Motion of Animals and Machines (pp. 131-142). Springer Tokyo.

Ounpuu, S., (1994). The biomechanics of walking and running. Clinics in sports medicine 13(4): 843-863.

Ozaki, T., Suzuki, T., Furuhashi, T., Okuma, S., Uchikawa, Y., (1991). Trajectory control of robotic manipulators using neural networks. Industrial Electronics, IEEE Transactions on 38(3): 195-202.

Park, J.H., Chung, S., (2011). Optimal locomotion trajectory for biped robot 'D2' with knees stretched, heel-contact landings, and toe-off liftoffs. Journal of mechanical science and technology 25(1): 3231-3241.

Pettersson, J., Sandholt, H., Wahde, M., (2001, November). A flexible evolutionary method for the generation and implementation of behaviors for humanoid robots. In Proc. of the IEEE-RAS International Conference on Humanoid Robots (pp. 279-286).

Pournazhdi, A.B., Mirzaei, M., Ghiasi, A.R., (2011, December). Dynamic modeling and sliding mode control for fast walking of seven-link biped robot. In Control, Instrumentation and Automation (ICCIA), 2011 2nd International Conference on (pp. 1012-1017). IEEE.

Pratt, J., Pratt, G., (1998, May). Intuitive control of a planar bipedal walking robot. In Robotics and Automation, 1998. Proceedings. 1998 IEEE International Conference on (Vol. 3, pp. 2014-2021). IEEE.

Saad, M., Dessaint, L.A., Bigras, P., Al-Haddad, K., (1994). Adaptive versus neural adaptive control: application to robotics. International journal of adaptive control and signal processing 8(3): 223-236.

Sangwan, V., Taneja, A., Mukherjee, S., (2004). Design of a robust self-excited biped walking mechanism. Mechanism and machine theory 39(12): 1385-1397.

Sanner, R.M., Slotine, J.J., (1992). Gaussian networks for direct adaptive control. Neural Networks, IEEE Transactions on 3(6): 837-863.

Singh, S., Mukherjee, S., Sanghi, S., (2008). Study of a self-impacting double pendulum. Journal of sound and vibration 318(4): 1180-1196.

Slotine, J.J.E., Li, W., (1987). On the adaptive control of robot manipulators. The International Journal of Robotics Research 6(3): 49-59.

Tzirkel-Hancock, E., Fallside, F., (1991, November). A direct control method for a class of nonlinear systems using neural networks. In Artificial Neural Networks, 1991., Second International Conference on (pp. 134-138). IET.

Vukobratovic, M., Borovav, B., Surla, D., Stokic, D., (1990). Biped Locomotion: Dynamics, Stability, Control and Application, Springer.

Wei, L.X., Yang, L., Wang, H.R., (2005, October). Adaptive neural network position/force control of robot manipulators with model uncertainties*. In Neural Networks and Brain, 2005. ICNN&B'05. International Conference on (Vol. 3, pp. 1825-1830). IEEE.

Yoshida, K., Kunimatsu, S., Ishitobi, M., (2012, August). Biped walking with stretched knee based on inverse kinematics via virtual prismatic joint and l∞ preview control. In SICE Annual Conference (SICE), 2012 Proceedings of (pp. 1870-1873). IEEE.

Zhihuan, Z., (2011, January). Free model control for semi-passive biped robot. In Measuring Technology and Mechatronics Automation (ICMTMA), 2011 Third International Conference on (Vol. 2, pp. 260-263). IEEE.

## APPENDIX A: GL Matrix and Operator

In this section, the definition of GL matrix, denoted by $\{\cdot\}$ and its product operator $\langle\bullet\rangle$ are briefly discussed. To avoid any possible confusion, $[\cdot]$ is used to denote the ordinary vector and matrix (Ge, 1996).

Let $I_0$ be the set of integers and $\theta_{kj}, \xi_{kj} \in R^{n_{kj}}$, where $n_{kj} \in I_0$, $j = 1,2,\ldots,n$, $k = 1,2,\ldots,n$. The GL row vector $\{\theta_k\}$ and its transpose $\{\theta_k\}^T$ are defined in the following way:

$$\{\theta_k\} = \{\theta_{k1} \quad \theta_{k2} \quad \cdots \quad \theta_{kn}\} \tag{A1}$$

$$\{\theta_k\}^T = \{\theta_{k1}^T \quad \theta_{k2}^T \quad \cdots \quad \theta_{kn}^T\} \tag{A2}$$

The GL matrix $\{\Theta_k\}$ and its transpose $\{\Theta_k\}^T$ are defined accordingly as

$$\{\Theta_k\} = \begin{Bmatrix} \theta_{11} & \theta_{12} & \cdots & \theta_{1n} \\ \theta_{21} & \theta_{22} & \cdots & \theta_{2n} \\ \vdots & \vdots & \vdots & \vdots \\ \theta_{n1} & \theta_{n2} & \cdots & \theta_{nn} \end{Bmatrix} = \begin{Bmatrix} \{\theta_1\} \\ \{\theta_2\} \\ \vdots \\ \{\theta_n\} \end{Bmatrix} \tag{A3}$$

$$\{\Theta_k^T\} = \begin{Bmatrix} \theta_{11}^T & \theta_{12}^T & \cdots & \theta_{1n}^T \\ \theta_{21}^T & \theta_{22}^T & \cdots & \theta_{2n}^T \\ \vdots & \vdots & \vdots & \vdots \\ \theta_{n1}^T & \theta_{n2}^T & \cdots & \theta_{nn}^T \end{Bmatrix} \tag{A4}$$

For a given GL matrix $\{\Xi\}$

$$\{\Xi\} = \begin{Bmatrix} \xi_{11} & \xi_{12} & \cdots & \xi_{1n} \\ \xi_{21} & \xi_{22} & \cdots & \xi_{2n} \\ \vdots & \vdots & \vdots & \vdots \\ \xi_{n1} & \xi_{n2} & \cdots & \xi_{nn} \end{Bmatrix} = \begin{Bmatrix} \{\xi_1\} \\ \{\xi_2\} \\ \vdots \\ \{\xi_n\} \end{Bmatrix} \tag{A5}$$

The GL product of $\{\Theta_k\}^T$ and $\{\Xi\}$ is $n \times n$ matrix defined as:

$$\left[\{\Theta_k\}^T \bullet \{\Xi_k\}\right] = \begin{bmatrix} \theta_{11}^T\xi_{11} & \theta_{12}^T\xi_{12} & \cdots & \theta_{1n}^T\xi_{1n} \\ \theta_{21}^T\xi_{21} & \theta_{22}^T\xi_{22} & \cdots & \theta_{2n}^T\xi_{2n} \\ \vdots & \vdots & \vdots & \vdots \\ \theta_{n1}^T\xi_{n1} & \theta_{n2}^T\xi_{n2} & \cdots & \theta_{nn}^T\xi_{nn} \end{bmatrix} \tag{A6}$$

The GL product of a square matrix and a GL row vector is defined as follows. Let $\Gamma_k = \Gamma_k^T = [\gamma_{k1} \quad \gamma_{k2} \quad \cdots \quad \gamma_{kn}], \gamma_{kj} \in R^{m \times n_{kj}}, m = \sum_{j=1}^{n} n_{kj}$ then we have:

$$\Gamma_k \bullet \{\xi_1\} = \{\Gamma_k\} \bullet \{\xi_1\} = [\gamma_{k1}\xi_{k1} \quad \gamma_{k2}\xi_{k2} \quad \cdots \quad \gamma_{kn}\xi_{kn}] \tag{A7}$$

Note that the GL product should be computed first in a mixed matrix product. For instance, in $\{A\} \bullet \{B\} C$ the matrix $\{A\} \bullet \{B\}$ should be computed first, and then follow by the multiplication of $\{A\} \bullet \{B\}$ with matrix $C$.